

**Anthropogenic Aerosols, Greenhouse Gases and the Uptake, Transport and Storage of Excess Heat in the Climate System**

D. B. Irving<sup>1</sup>, S. Wjiffels<sup>1,2</sup>, and J. A. Church<sup>3</sup>

<sup>1</sup>CSIRO Oceans and Atmosphere, Hobart, Tasmania, Australia

<sup>2</sup>Woods Hole Oceanographic Institution, Woods Hole, Massachusetts, USA

<sup>3</sup>Climate Change Research Centre, University of New South Wales, Sydney, New South Wales, Australia

**Contents of this file**

Table S1

Text S1

Figure S1-6

**Introduction**

In order for a model (details in Table S1) to be included in our study, we required closure of the global excess energy budget. The relevant budget terms are plotted in Figure S1 for each model/experiment, while Text S1 describes how the ocean surface heat uptake was calculated for the model that did not archive the relevant variable.

Figures S2 and S3 demonstrate that the hemispheric distribution and meridional patterns of excess heat uptake, transport and storage for the 1pctCO<sub>2</sub> experiment was very similar to the GHG-only experiment.

Figure S4 demonstrates that the interhemispheric temperature difference results presented in the manuscript (Figure 2) are consistent with those obtained from a larger ensemble of CMIP5 models.

Figure S5 shows that the zonally integrated excess heat uptake and storage for the GHG-only and AA-only experiments was approximately linearly additive (i.e. their linear sum closely resembles the historical experiment), while Figure S6 shows this same zonally integrated picture out to the year 2100 for the RCP 8.5 experiment.

Model	Atmosphere grid		Ocean grid		AA-only	Branch time	
	Lat	Lon	Lat	Lon		historical	1pctCO2
CanESM2	2.8	2.8	0.9, 1.1	1.4	r1i1p4	171915	
CCSM4	0.9	1.25	lat(i,j)	lon(i,j)	r1i1p10	342005	91615
CSIRO-Mk3-6-0	1.9	1.9	0.9	1.9	r1i1p4	29200	37595
FGOALS-g2	2.8	2.8	0.5, 1.0	1.0	r2i1p1	175382	
GISS-E2-R	2.0	2.5	1.0	1.3	r1i1p107	0 (after year 3981)	
NorESM1-M	1.9	2.5	lat(i,j)	lon(i,j)	r1i1p1	255151	

**Table S1.** Details of the CMIP5 the models used in the study. If two values are given for the latitude resolution of the ocean grid, resolution is not constant. The first value is that for the equator, the second for the poles (maximum for the two poles if different). In case of rotated poles the resolutions for the rotated coordinates rlon and rlat are tabulated. lat(i,j) and lon(i,j) denote latitudes and longitudes defined with two indices i and j. In this case the resolution cannot simply be read out. Details of the model run used for the AA-only experiment (a subset of historicalMisc) are shown. For all other experiments (historical, historicalGHG, rcp85, 1pctCO2) r1i1p1 was used. All historical experiments (i.e. historical, historicalGHG and historicalMisc) share the same branch time. There is a time discontinuity in the GISS-E2-R control run, so data prior to that discontinuity (i.e. prior to year 3981) was not used.

**Text S1.**

The downward heat flux at sea water surface (hfds) variable was not archived for the CanESM2 model, however we were able to infer it from the remaining surface fluxes: surface upward sensible heat flux (hfss), surface upward latent heat flux (hfls), heat flux into sea water due to sea ice thermodynamics (hfsitherm ds), surface downwelling shortwave flux in air (rsds), surface upwelling shortwave flux in air (rsus), surface downwelling longwave flux in air (rlds) and surface upwelling longwave flux in air (rlus).

The calculation involved balancing the net radiative flux with the sum of the surface heat fluxes, adjusted for the contribution from sea ice thermodynamics:

$$hfds + hfss + hfls + hfitherm ds = (rsds - rsus) + (rlds - rlus)$$

or equivalently,

$$hfds = (rsds - rsus) + (rlds - rlus) - hfss - hfls + hfitherm ds$$

Since most models archive all of the variables listed above except hfitherm ds, we experimented with setting hfitherm ds to zero in other models (i.e. as a solution for expanding the ensemble to all models that did not archive hfds). Unfortunately, the resulting non-closure between the OHU and netTOA/OHC terms was regularly greater than 70%, which indicates that hfitherm ds is a required variable.

The CanESM2 sea ice thermodynamics are documented in detail by McFarlane et al (1992).

McFarlane, N. A., Boer, G. J., Blanchet, J.-P., & Lazare, M. (1992). The Canadian Climate Centre second-generation general circulation model and its equilibrium climate. *Journal of Climate*, 5(10), 1013–1044.

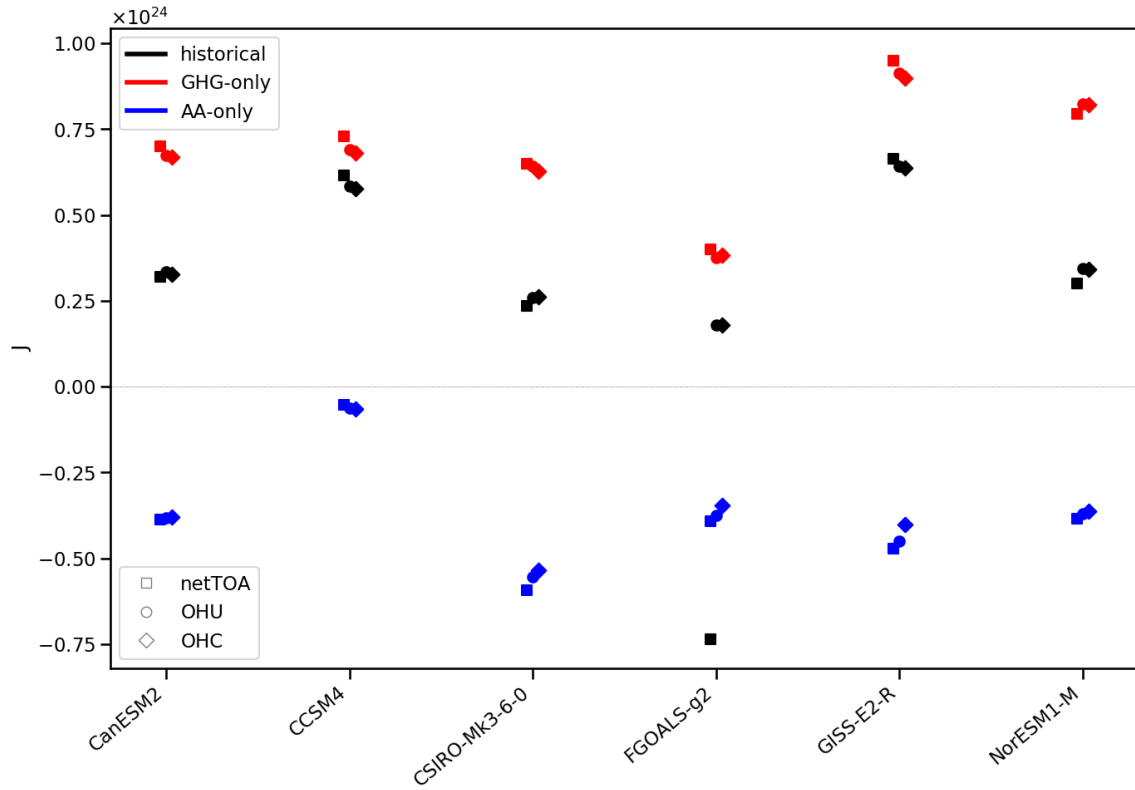


**Figure S1.** Globally accumulated uptake and storage of excess heat over the period 1861-2005. The accumulated net radiative flux anomaly at the top of the atmosphere (netTOA), accumulated heat flux anomaly at the ocean surface (ocean heat uptake; OHU) and change in ocean heat storage (ocean heat content; OHC) are shown for each model/experiment.

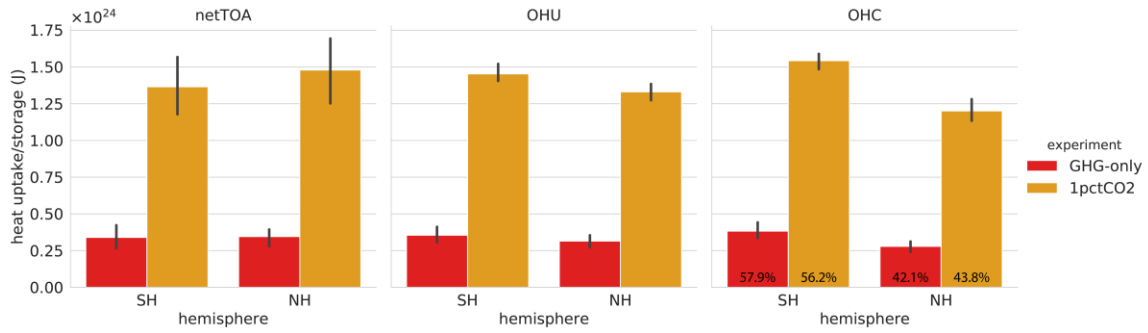


**Figure S2.** Total hemispheric uptake and storage of excess heat over the period 1861-2000 for the GHG-only and 1pctCO<sub>2</sub> experiments. Ensemble mean values (and the 95% confidence interval) are shown for the accumulated net radiative flux anomaly at the top of the atmosphere (netTOA), accumulated heat flux anomaly at the ocean surface (ocean heat uptake; OHU) and change in ocean heat storage (ocean heat content; OHC). The percentage of global excess heat stored in either hemisphere is indicated for both experiments (the GHG-only percentages differ slightly from Figure 1 because a slightly shorter time period is used here to match the 1pctCO<sub>2</sub> experiment).

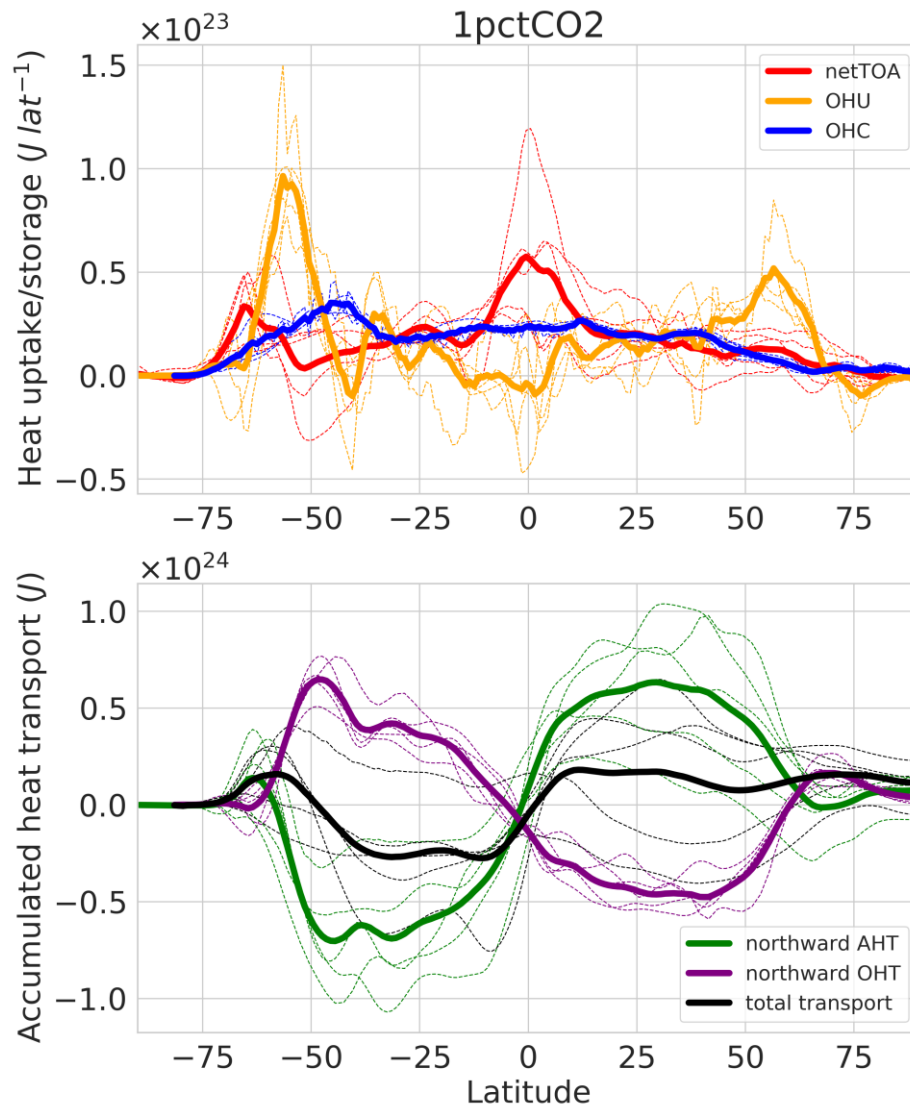


**Figure S3.** Zonally integrated uptake, transport and storage of excess heat over the period 1861-2000 for the 1pctCO<sub>2</sub> experiment. Thick lines indicate the ensemble mean, while each of the individual models are shown in thin dashed lines. The top row shows the accumulated net radiative flux anomaly at the top of the atmosphere (netTOA), accumulated heat flux anomaly at the ocean surface (ocean heat uptake; OHU) and change in ocean heat content (OHC), while the bottom row shows the accumulated northward oceanic heat transport (OHT), atmospheric heat transport (AHT) and total heat transport inferred from those values.

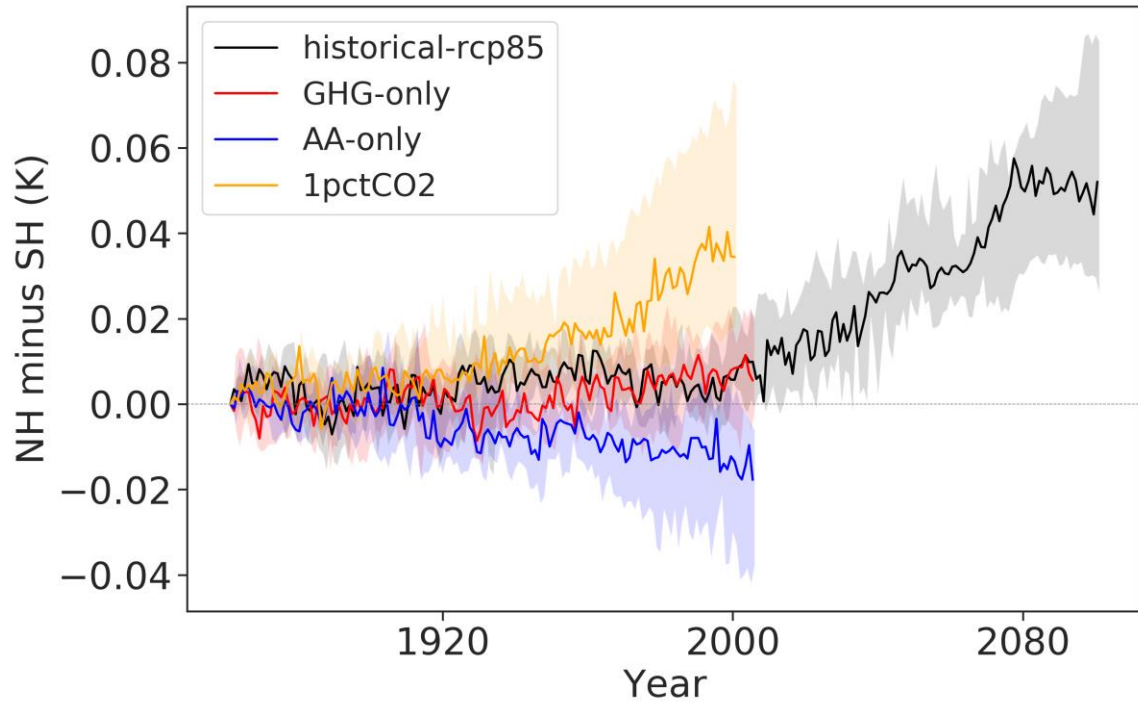


**Figure S4.** Interhemispheric difference in (volume weighted) average ocean temperature (NH minus SH). The annual mean temperature difference anomaly is shown, where solid lines represent the ensemble median and the shading spans the ensemble interquartile range. As opposed to the five member ensemble used for the remainder of the study, the ten models that performed all the experiments of interest are included here (CanESM2, CCSM4, CSIRO-Mk3-6-0, FGOALS-g2, GFDL-CM3, GFDL-ESM2M, GISS-E2-R, GISS-E2-H, IPSL-CM5A-LR and NorESM1-M).

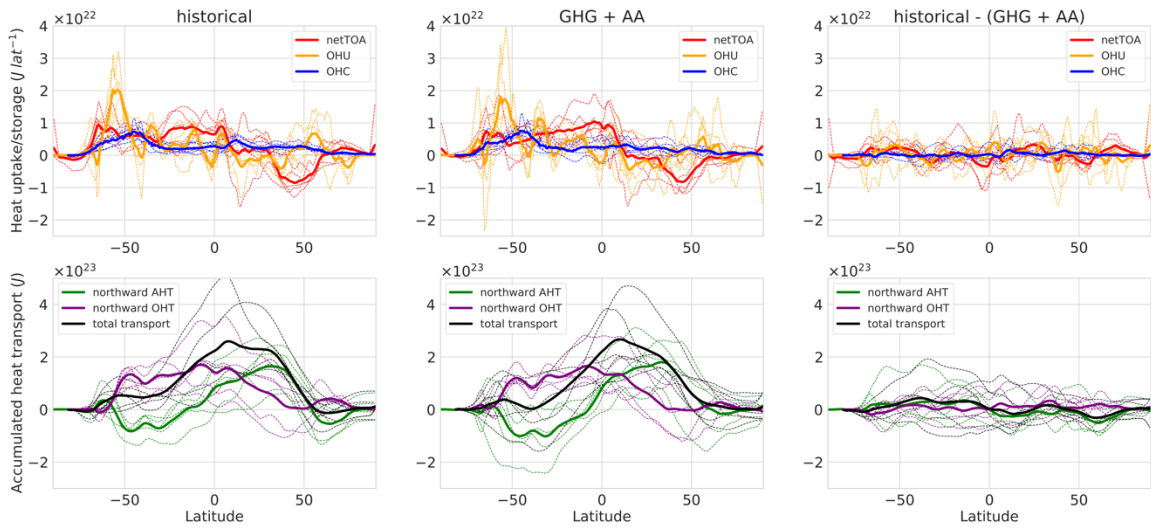


**Figure S5.** As per Figure S3 but for the 1861-2005 period. The historical experiment (left column), GHG-only experiment minus AA-only experiment (center column) and the historical experiment minus the sum of the GHG-only and AA-only experiments (right column) is shown.

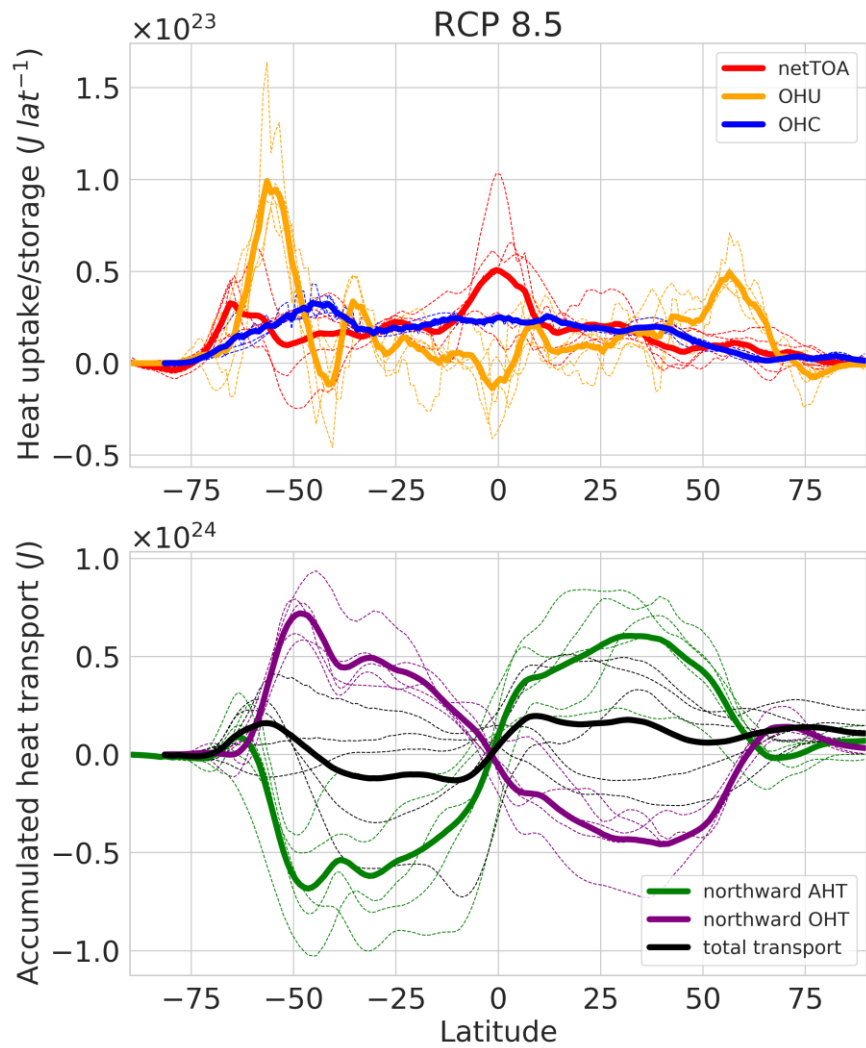


**Figure S6.** As per Figure S3 but for the 2006-2100 period, RCP 8.5 experiment.